

## SUPPLEMENTAL APPENDIX

### **Correlation of immune fitness with response to teclistamab in relapsed/refractory multiple myeloma in the MajesTEC-1 study**

Diana Cortes-Selva,<sup>1</sup> Tatiana Perova,<sup>1</sup> Sheri Skerget,<sup>1</sup> Deeksha Vishwamitra,<sup>1</sup> Sarah Stein,<sup>1</sup> Rengasamy Boominathan,<sup>1</sup> Onsay Lau,<sup>1</sup> Karl Calara-Nielsen,<sup>1</sup> Cuc Davis,<sup>1</sup> Jaymala Patel,<sup>1</sup> Arnob Banerjee,<sup>1</sup> Tara Stephenson,<sup>1</sup> Clarissa Uhlar,<sup>1</sup> Rachel Kobos,<sup>2</sup> Jenna Goldberg,<sup>2</sup> Lixia Pei,<sup>2</sup> Danielle Trancucci,<sup>2</sup> Suzette Girgis,<sup>1</sup> Shun Xin Wang Lin,<sup>1</sup> Liviawati S. Wu,<sup>3</sup> Philippe Moreau,<sup>4</sup> Saad Z. Usmani,<sup>5</sup> Nizar J. Bahlis,<sup>6</sup> Niels W.C.J. van de Donk,<sup>7</sup> and Raluca I. Verona<sup>1</sup>

<sup>1</sup>Janssen Research & Development, Spring House, PA; <sup>2</sup>Janssen Research & Development, Raritan, NJ; <sup>3</sup>Janssen Research & Development, South San Francisco, CA; <sup>4</sup>University Hospital Hôtel-Dieu, Nantes, France; <sup>5</sup>Memorial Sloan Kettering Cancer Center, New York, NY; <sup>6</sup>Arnie Charbonneau Cancer Institute, University of Calgary, Calgary, AB, Canada; <sup>7</sup>Amsterdam University Medical Center, Vrije Universiteit Amsterdam, Amsterdam, The Netherlands

## Methods

### *Analyses of bone marrow and peripheral blood samples using flow cytometry*

Peripheral blood was collected prior to step-up dose 1. Bone marrow samples analyzed by flow cytometry were collected at baseline and at cycle (C) 3 day (D) 1. Baseline frequency and density of membrane-bound B-cell maturation antigen (BCMA) was performed using CD138+ enriched plasma cells from bone marrow by staining with the following antibodies: CD45 (clone: 2D1, BD Biosciences), fixable viability dye eFluor506 (eBiosciences), CD38 (clone: Humab-003, JnJ), CD138 (DL-101, Biolegend), CD269 BCMA (clone: 19F2, Biolegend). Receptor density assessment was performed using AF647 Quantum beads (Bang Laboratories).

Immunophenotyping profiling was performed in a BD FACSCelesta (BD Biosciences), and data were analyzed in FlowJo (V10.6.2). Measurement of immune markers in T cells from peripheral blood mononuclear cells (isolated using Ficoll Paque™ PREMIUM density gradient centrifugation) was performed using the following antibodies: PD-1 (EH12.1, BD Biosciences), TIM-3 (7D3, BD Biosciences), CD3 (UCHT1, BD Biosciences), CD38 (Humab-003, Janssen), CD25 (M-A251, BD Biosciences), CD4 (RPA-T4, BD Biosciences), CD8 (SK1, BD Biosciences), CD127 (eBioRDR5, ThermoFisher), CD45RA (HI100, BD Biosciences), CD45RO (UCHL1, BD Biosciences), and eFluor506 Fixable Viability Dye (ThermoFisher) to assess viability. In order to prevent nonspecific binding of antibodies, a Fc blocking reagent (FC Block, ThermoFisher) was added. Sample acquisition was performed in a BD LSR Fortessa X-20 (Becton Dickinson) cytometer. Quantitation of cell populations was performed using an off-the-shelf TBNK kit assay (BD Biosciences) according to the manufacturer's instructions. Maximal fold change analyses for induction of T-cell activation in the bone marrow in response to treatment were calculated at C3D1 (pre dose) and compared with baseline.

*Analyses of bone marrow and peripheral blood samples using cytometry by time of flight (CyTOF)*

Peripheral blood samples were collected and fixed in Smart Tubes<sup>®</sup> (Smart Tube, Inc.) for 10 minutes at room temperature and stored at  $-80^{\circ}\text{C}$  until analysis. CyTOF profiling was evaluated from active dose cohorts. Samples were collected at baseline (27 from responders and 13 from nonresponders). Additionally, bone marrow samples collected at baseline from 52 patients in the pivotal RP2D study population were profiled using CyTOF (24 from responders and 28 from nonresponders). For bone marrow samples, CD138-depleted fraction-viable, cryopreserved bone marrow samples were used.

Two panels of 45 and 38 antibodies were used for analysis of the peripheral blood and bone marrow samples, respectively (**Supplemental Tables 1 and 2**). Antibodies preconjugated to metal isotopes were purchased from Standard Bio Tools. Additional antibodies were purchased from other vendors and conjugated to metal isotopes using the Maxpar<sup>®</sup> Antibody Labeling Kit (Standard Bio Tools) according to the manufacturer's protocol.

The frozen Smart Tube whole blood samples were thawed in a water bath at  $10^{\circ}\text{C}$  for 20 minutes, then 3 mL of 1 $\times$  Thaw-Lyse buffer (Smart Tube) was added, mixed, and strained through a 70- $\mu\text{M}$  strainer (MACS SmartStrainer, Miltenyi Biotec Inc.). The strainer was washed with 40 mL of 1 $\times$  Thaw-Lyse buffer and incubated at room temperature for 10 minutes for lysing red blood cells. The samples were centrifuged (600 g, 5 minutes,  $20^{\circ}\text{C}$ ), and pellets were resuspended in 1 $\times$  BD lysing buffer (BD Biosciences) and incubated for 10 minutes at room temperature for additional red blood lysis. After centrifugation, the pellets were resuspended in 100  $\mu\text{L}$  of stain buffer, and the samples were purified using CD235 microbeads for negative selection, a method in accordance with the manufacturer's protocol. The purified samples were barcoded using the Standard Bio Tools Cell-ID 20-Plex Pd barcoding kit. Individual samples were washed, resuspended in 1 $\times$  barcode perm wash buffer (Standard Bio Tools), and

incubated for 30 minutes at room temperature. After incubation, the samples were centrifuged (600 g, 5 minutes, 20°C), washed with stain buffer, and pooled. The pooled samples were incubated with TruStain FcX (BioLegend) for 30 minutes at room temperature to block surface Fc receptors. After washing off the TruStain FcX blocker, the cells were stained with a mixture of surface antibodies and incubated at room temperature for 30 minutes. Cells were washed with staining buffer, resuspended in BD Cytfix/Cytoperm (BD Biosciences), and incubated on ice for 20 minutes. After incubation, cells were washed with 1× BD Perm/Wash buffer (BD Biosciences), resuspended in the intracellular staining antibody mixture, and incubated on ice for 30 min. After washing with 1× BD Perm/Wash buffer, the cell pellets were resuspended in phosphate buffered saline (PBS) with saponin (0.3%) containing formaldehyde (1.6%) and 125 μM Ir intercalator (Cell-ID™ Intercalator-Ir–125 μM, Standard Bio Tools) and incubated at 4°C overnight.

Bone marrow (frozen viable) samples, depleted of CD138+ cells, were thawed and immediately transferred to 5 mL of media and centrifuged. After centrifugation and 15-minute TruStain FcX incubation, washing and surface-staining incubation for 35 minutes was performed. Samples were then barcoded using the Standard Bio Tools Cell-ID 20-Plex Pd barcoding kit. After barcoding, samples were pooled, and intracellular staining using a transcription factor buffer set (BD Biosciences) was performed according to the manufacturer's instructions. After washing, cell pellets were resuspended in PBS with saponin (0.3%) containing formaldehyde (1.6%) and 125- μM Ir intercalator (Cell-ID™) and incubated at 4°C overnight.

#### *CyTOF data acquisition and processing*

After overnight incubation, stained cells were washed with staining buffer and subsequently washed in Maxpar Cell Acquisition Solution (CAS) (Standard Bio Tools) to remove buffer salts.

Then the cells were resuspended in CAS with a 1:10 dilution of EQ Four Element Calibration beads (Standard Bio Tools) and filtered through a 35- $\mu$ m nylon mesh filter cap (Falcon). Samples were analyzed on a Helios 2 CyTOF mass cytometer (Standard Bio Tools). Each experiment included whole blood samples from 2 healthy donors for quality control purposes. In total, for peripheral blood samples, 16 experiments were run and each of them was considered a batch. For bone marrow samples, 5 experiments were run and each considered a batch. Data acquired on CyTOF were obtained in FCS file format and normalized using CyTOF Software 7.0.8493 for Stand-Alone Processing Workstations (Standard Bio Tools). Manual gating of immune populations was performed using Cytobank software v10.2 (Beckman Coulter). Cell clustering was performed on Cytobank using the high dimensional population identification tool SPADE (Spanning-tree Progression Analysis of Density-normalized Events). Through manual review of marker expression on the tree, known immune cell subsets were identified as “bubbles”. Following this, a hypothesis-generating approach was employed to identify any trends in the data in an unbiased way. These data analyses were performed using in-house scripts and the R 4.0.2 and RStudio 1.1.442 software.

Quality control for peripheral blood and bone marrow was performed using the HilbertSimilarity distance (Abraham Y, et al. <https://zenodo.org/record/3557362#.YmayldrMJPY>. Accessed April 25, 2022), Earth Mover’s Distance (Qiu P. *PLoS One*. 2012;7:e37038), and marker enrichment modeling (Diggins KE, et al. *Nat Methods*. 2017;14:275-278) algorithms.

#### *Differential analysis of cell proportions derived from unsupervised CyTOF data*

Differences in population size were assessed by fitting a generalized linear mixed-effects model for the negative binomial family with the following formula:  $N \sim ORR * TimePoint + (1|SUBJID) + offset(\log(Total))$ , where  $N$  corresponds to the population size,  $ORR$  refers to the overall

response rate (ie, either responders, R, or nonresponders, NR), and  $(1/SUBJID)$  accounts for the random effect given by the subject. These differences were assessed for all cell populations' definitions (ie, clusters, bubbles and manually gated populations). The (R-NR) baseline contrast was included in the analysis. Multiple testing correction was performed per population definition at two levels: over all contrasts, using SIDAK, and over all populations using the false-discovery rate. Results were flagged as significant when the corrected  $P$ -value was smaller than 0.05, and the absolute estimated change was bigger than 1.

CD8 and CD4 T-cell subsets identified through bubble annotation of the SPADE tree were visualized using FreeViz projections, and further analyzed using a supervised learning approach to identify any difference in cellular composition driven by response to treatment, as previously described (Verkleij CPM, et al. *HemaSphere*. 2023;7:e881 and Qing M, et al. *Ann Hematol*. 2024;Jan 18 [online ahead of print; doi: 10.1007/s00277-023-05603-w]).

#### *Baseline serum soluble BCMA (sBCMA) quantitation*

Serum was collected prior to the first teclistamab dose. Serum samples were analyzed for sBCMA using an electrochemiluminescence ligand-binding assay (ECLIA) using the Meso Scale Discovery (MSD) platform. Briefly, the assay uses a biotin-labeled, antihuman BCMA antibody and a Sulfo-tag (ruthenium)-labeled antihuman BCMA antibody mixed with serial dilutions of serum samples, and then added to a streptavidin-MSD plate. Electricity is applied to the plate electrodes by an MSD instrument leading to light emission by Sulfo-tag labels. Light intensity is then measured to quantify analytes in the sample. The lowest quantifiable detection value of the assay was defined as 1.0 ng/mL.

### *Baseline cytokine analysis*

Serum baseline samples were collected before the first step-up dose. Frozen serum samples at baseline were assessed using MSD (ECLIA) or bead-based immunoassay. For MSD assays, 2 commercially available kits were used: Proinflammatory Panel 1 (V-PLEX PLUS Human Kit, catalog #K15049G), which measures 10 cytokines (interferon [IFN]- $\gamma$ , interleukin [IL]-1 $\beta$ , IL-2, IL-4, IL-6, IL-8, IL-10, IL-12p70, IL-13, and tumor necrosis factor [TNF]- $\alpha$ ) and the U-PLEX Human Kit (catalog #K151XGK), which measures IL-2R $\alpha$ . Assays were performed according to the manufacturer's recommendations. For bead-based immunoassay, quantitative multiplex bead assay methodology using Luminex technology, (Cytokine Panel 13, Serum, ARUP Test #0051394) was used according to the manufacturer's experimental procedures. This kit includes the following analytes: IFN-  $\gamma$ , IL-1B, IL-2, IL-2R, IL-4, IL-5, IL-6, IL-8, IL-10, IL-12, IL-13, IL-17, and TNF- $\alpha$ .

### *Statistical analysis*

Responders and nonresponders were classified using the best response per independent review committee (IRC) when available, otherwise the best response per investigator was used.

Patients were classified as responders if their best response was partial response or better.

Percent plasma cells by bone marrow biopsy or aspirate at baseline was used to determine tumor burden and classify patients as having <60% or  $\geq$ 60% bone marrow plasma cells (BMPCs).

A composite tumor burden classification was also implemented that assessed plasmacytosis, serum M-spike, and serum free light chain levels. Patients were classified as having high composite tumor burden if they had any of the following characteristics: BMPCs  $\geq$ 80%, serum M-spike  $\geq$ 5 g/dL, or serum free light chain  $\geq$ 5000 mg/L. Patients were classified as having low

composite tumor burden when all of the following parameters, as applicable to the patient, were met: BMPCs <50%, serum M-spike <3 g/dL, serum free light chain <3000 mg/L. Finally, patients who did not fit the criteria for the high or low groups were classified as having intermediate composite tumor burden. Binomial logistic regression analysis to examine the prognostic value of sBCMA as well as other indicators of high-risk disease including BMPC %, lactate dehydrogenase level, beta-2 microglobulin level, International Staging System (ISS) stage III, revised ISS stage III, and presence of extramedullary plasmacytomas in predicting response was performed in 142 patients (patients missing values from any of the parameters mentioned above were removed from the analysis). For continuous variables, the Shapiro-Wilk test was performed to evaluate normality. None of the continuous variables were found to follow a normal distribution and were thus  $\log_{10}(\text{value} + 1)$  transformed. A binomial regression analysis was found to be significantly associated with response if  $P < 0.05$ .

All bioinformatic analyses were performed in R (v4.0.5). The Wilcoxon rank-sum test was performed to identify relevant immune correlates that differed between responders and nonresponders, and a Spearman correlation test was performed to investigate their relationship with tumor burden (percentage of BMPCs) to assess correlates indicative of response independently of disease burden. Additionally, we calculated the Benjamini-Hochberg (BH)-corrected  $P$ -value, accounting for the 38 different flow cytometry markers. Due to the large number of markers included in this exploratory analysis, none of the BH-adjusted  $P$ -values met a  $P < 0.05$  significance threshold. We included in the exploratory analysis the frequency of several T-cell subsets and biomarkers that are indicative of T-cell function, which may be key to inform mechanisms of action.

Unpaired, 2-sided Wilcoxon rank-sum tests were performed using `wilcox.test`, Kruskal-Wallis rank-sum tests were performed using `kruskal.test`, and analysis of variation (ANOVA) tests were

performed using aov from the stats package. Maximum fold change from baseline values were based on observations between C3D1 and baseline.

Survival curves were estimated using the Kaplan-Meier method implemented by survfit from the survival package (R v.3.2-10) and visualized using ggsvplot from the survminer (0.4.9) package. Median time to event was based on progression-free survival as determined by IRC. Cox proportional hazards models were calculated using coxph from the survival package.

Regression plots were generated by fitting a linear model using geom\_smooth from the ggplot2 (3.4.0) package. Two-sided Pearson correlation coefficients and *P*-values were calculated using stat\_cor from the ggpubr (0.4.0) package.

**Supplemental Table 1. Antibody panel for CyTOF analysis of peripheral blood samples.**

<b>Specificity</b>	<b>Clone</b>	<b>Metal isotope</b>	<b>Purpose</b>	<b>Type</b>
CD45	HI30	89Y	Leukocytes	Phenotypic
IgLambda	MHL-38	111Cd	B cells, myeloma cells	Functional
CD39	Clone A 1	112Cd	B cells, T cells	Phenotypic
CD66b	80H3	113Cd	Granulocytes	Phenotypic
Active caspase 3	C92-605	141Pr	Apoptotic cells	Reference
CD20	2H7	142Nd	B lymphocytes	Phenotypic
CD3	UCHT1	143Nd	T lymphocytes	Phenotypic
CD11b	ICRF44	144Nd	Monocytes, NK cells	Phenotypic
CD4	RPA-T4	145Nd	T-helper lymphocytes	Phenotypic
CD8	RPA-T8	146Nd	Cytotoxic T lymphocytes	Phenotypic
CD24	ML5	147Sm	Regulatory B cells	Phenotypic
CD127	eBioRDR5	148Nd	Activated and regulatory T cells	Phenotypic
CD45RO	UCHL1	149Sm	Memory T lymphocytes	Phenotypic
CD138	MI15	150Nd	Plasma cells, multiple myeloma cells	Functional
CD33	WM53	151Eu	Myeloid cells	Phenotypic
CD55	MEM118	152Sm	Complement inhibition	Functional
CD366 (TIM-3)	344823	153Eu	Effector T cells, T-cell exhaustion	Functional
CD45RA	HI100	154Sm	Naive T lymphocytes	Phenotypic
CD27	L128	155Gd	Memory B lymphocytes, T lymphocytes	Phenotypic
CD152 (CTLA4)	L3D10	156Gd	Regulatory T cells, T-cell activation	Functional
CD137	4B4-1	158Gd	Activated NK cells	Functional
CD123	9F5	159Tb	Plasmacytoid dendritic cells, basophils	Phenotypic
CD69	FN50	160Gd	T-cell early activation	Functional
CD28	CD28.2	161Dy	T-cell co-stimulation	Phenotypic
CD11c	Bu15	162Dy	Monocytes, myeloid dendritic cells	Phenotypic
Granzyme B	GB11	163Dy	Activated T cells, NK cells	Phenotypic
CD15	W6D3	164Dy	Granulocytes	Phenotypic
CD80	MM0100-6N36	165Ho	Antigen-presenting cells, CD28, and CTLA4 ligand	Functional
GPRC5D	571961	166Er	Plasma cells	Functional
CD19	HIB19	167Er	B lymphocytes	Phenotypic
CD269 (BCMA)	Vicky	168Er	Plasma cells	Functional

CD25	M-A251	169Tm	Activated and regulatory T lymphocytes	Phenotypic
CD279 (PD-1)	EH12-1	170Er	T-cell co-inhibitory receptor/exhaustion	Functional
CD14	HCD14	171Yb	Monocytes, macrophages	Phenotypic
CD38	HuMax	172Yb	Activation, plasma cells	Functional
CD223 (LAG3)	17B4	173Yb	T-cell co-inhibitory receptor	Functional
HLA-DR	646-6	174Yb	Dendritic cells, monocytes, B lymphocytes, T-cell activation	Phenotypic
CD274 (PD-L1)	29E.2A3	175Lu	Activation PD-1	Functional
CD56	R19-760	176Yb	NK and NKT cells	Phenotypic
DNA	Intercalator	191Ir, 193Ir	Nucleated cells	DNA
CD95	DX2	195Pt	Blast cells	Functional
IgKappa	MHK-49	196Pt	Myeloma cells	Functional
CD117	104D2	198Pt	Germ cells, hematopoietic stem cells	Functional
CD16	3G8	209Bi	Proinflammatory monocytes, NK subset, granulocytes	Phenotypic

---

BCMA, B-cell maturation antigen; CTLA4, cytotoxic T-lymphocyte-associated protein 4; CyTOF, cytometry by time of flight; GPRC5D, G protein-coupled receptor family C group 5 member D; HLA-DR, human leukocyte antigen DR; Ig, immunoglobulin; LAG3, lymphocyte activation gene-3; NK, natural killer; NKT, natural killer T cell; PD-1, programmed death-1; PD-L1, programmed death ligand-1; TIM-3, T-cell immunoglobulin mucin-3.

**Supplemental Table 2. Antibody panel for CyTOF analysis of bone marrow samples.**

<b>Specificity</b>	<b>Clone</b>	<b>Metal isotope</b>	<b>Purpose</b>	<b>Type</b>
CD45	HI30	89Y	Leukocytes	Reference
TCRgd	B1	175Lu	$\gamma\delta$ T cells	Phenotypic
FoxP3	PCH101	162Nd	Transcription factor	Phenotypic
CD28	CD28.2	142Nd	Co-stim, development and survival	Functional
CD3	UCHT1	170Er	T lymphocytes	Phenotypic
CD4	RPA-T4	176Yb	T-helper lymphocytes	Phenotypic
CD8	RPA-T8	146Nd	Cytotoxic T lymphocytes	Phenotypic
Perforin	dG9	152Sm	Cytolytic cytokine	Functional
CD127	eBioRDR5	166Er	Activated and regulatory T cells	Phenotypic
CCR7	150503	172Yb	Activated, memory cells	Phenotypic
CCR4	L291H4	149Sm	Treg effector typr	Phenotypic
Nrp1	12C2	151Eu	Treg stability, checkpoint	Functional
OX40	ACT35	156Gd	Co-stim factor, survival and proliferation	Functional
CD366 (TIM-3)	344823	161Dy	Effector T cells, T-cell exhaustion	Functional
CD45RA	HI100	153Eu	Naive T lymphocytes	Phenotypic
CD27	L128	155Gd	Memory B lymphocytes, T lymphocytes	Phenotypic
CD152 (CTLA4)	L3D10	160Gd	Regulatory T cells, T-cell activation	Functional
CD137	4B4-1	167Er	Activated NK cells	Functional
CD314 (NKG2D)	1D11	158Gd	NK-associated activating receptor	Functional
CD69	FN50	144Nd	T-cell early activation	Functional
Granzyme B	GB11	141Pr	Activated T cells, NK cells	Functional
CD73	AD2	173Yb	Immunomodulatory in lymphocytes	Functional
TIGIT	A15153G	116Cd	Checkpoint marker	Functional
CD278	C398.4A	148Nd	Co-stim molecule, activated T cells	Functional
CD25	M-A251	169Tm	Activated and regulatory T lymphocytes	Phenotypic
CD279 (PD-1)	EH12-1	145Nd	T-cell co-inhibitory receptor/exhaustion	Functional
CD161	HP-3G10	168Er	Cytokine-producing Tregs, NK activation receptor	Functional
CD38	240742	165Ho	Activation, plasma cells	Functional
CD223 (LAG3)	17B4	147Sm	T-cell co-inhibitory receptor	Functional
HLA-DR	L243	174Yb	Dendritic cells, monocytes, B lymphocytes, T-cell activation	Functional
CD57	NK-1	154Sm	Activation marker in NK cells	Phenotypic

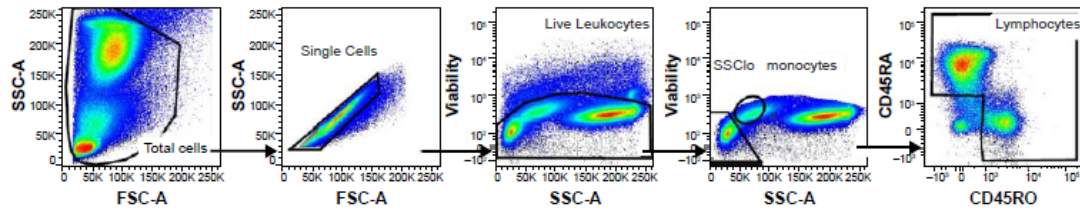
CD56	R19-760	163Dy	NK and NKT cells	Phenotypic
DNA	Intercalator	191Ir, 193 Ir	Nucleated cells	DNA
Ki67	Ki-67	164Dy	Proliferating cells	Functional
CD39	A 1	143Nd	B cells, T cells	Functional
CD16	3G8	209Bi	Proinflammatory monocytes, NK subset, granulocytes	Phenotypic
NKp30	210845	171Yb	NK-associated activating receptor	Functional
NKp44	p44-8	159Tb	NK-associated activating receptor	Functional
NKp80	5D12	150Nd	NK-associated activating receptor	Functional
CD19, CD138, CD66b, CD14	HIB19 MI15 913542 M5E2	112Cd	Dump (B cells, plasma cells, granulocytes, myeloid lineage)	Reference

---

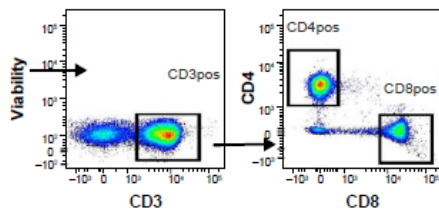
CCR4, C-C motif chemokine receptor 4; CCR7, C-C motif chemokine receptor 7; CTLA4, cytotoxic T-lymphocyte-associated protein 4; CyTOF, cytometry by time of flight; HLA-DR, human leukocyte antigen DR; LAG3, lymphocyte activation gene-3; NK, natural killer; NKG2D, natural killer group 2D receptor; NKT, natural killer T cell; Nrp1, neuropilin 1; PD-1, programmed death-1; TCRgd, T-cell receptor gamma delta T cell; TIGIT, T-cell immunoglobulin and ITIM domain; TIM-3, T-cell immunoglobulin mucin-3; Treg, immunosuppressive regulatory T cell.

**Supplemental Figure 1. Gating strategy for T-cell phenotypes identified by flow cytometry in peripheral blood.**

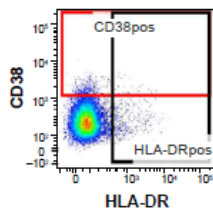
**Flow cytometry gating strategy**



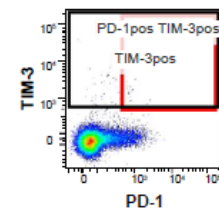
**CD3 T cells**



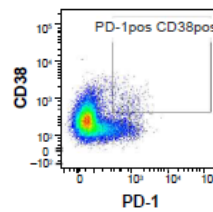
**CD4 subsets**



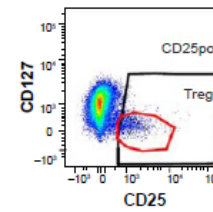
CD38+  
CD4 T cells



PD-1+ TIM-3+  
CD4 T cells

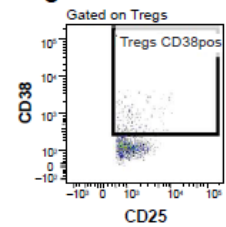


PD-1+ CD38+  
CD4 T cells



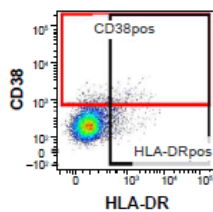
CD25+  
CD4 T cells

**Tregs**

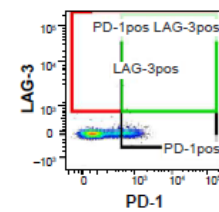


CD38+  
Tregs

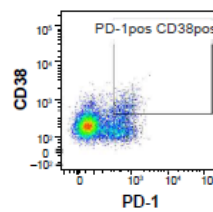
**CD8 subsets**



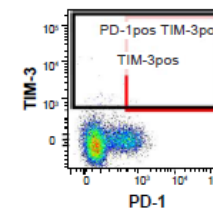
CD38+  
CD4 T cells



PD-1+  
CD8 T cells



PD-1+ CD38+  
CD8 T cells



PD-1+ TIM-3+  
CD8 T cells

Representative dot plots show the gating strategy for measuring circulating T-cell subsets.

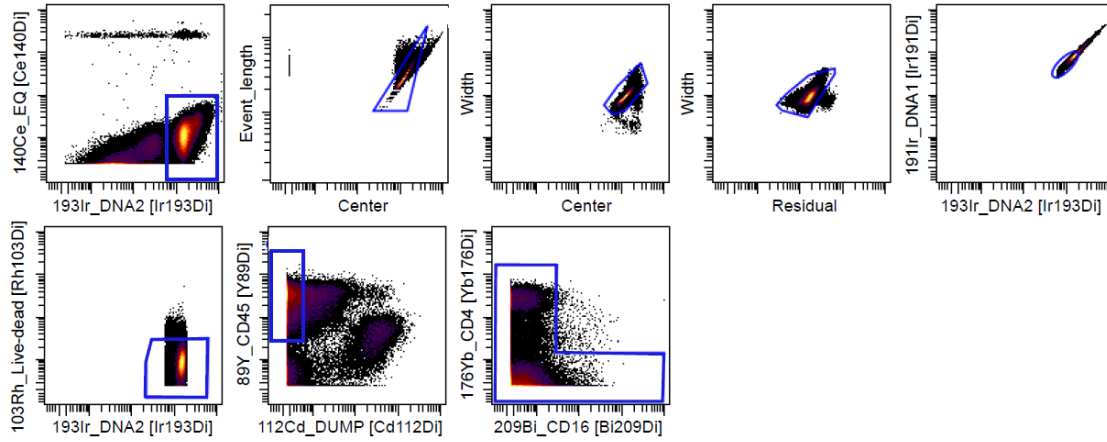
Following the exclusion of dead cells and doublets, CD4 T cells were identified as

CD45+CD3+CD8-CD4+ and CD8 T cells were identified as CD45+CD3+CD8+CD4-.

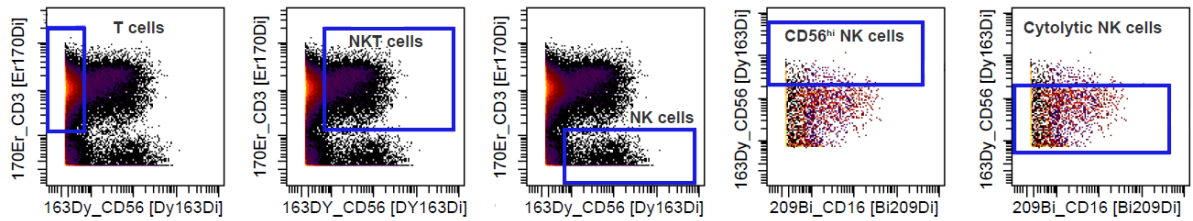
Tregs were defined as CD45+CD3+CD8-CD4+CD127-CD25+. Treg, regulatory T cell.

**Supplemental Figure 2. Gating strategy for immune cell phenotypes identified by mass cytometry in bone marrow.**

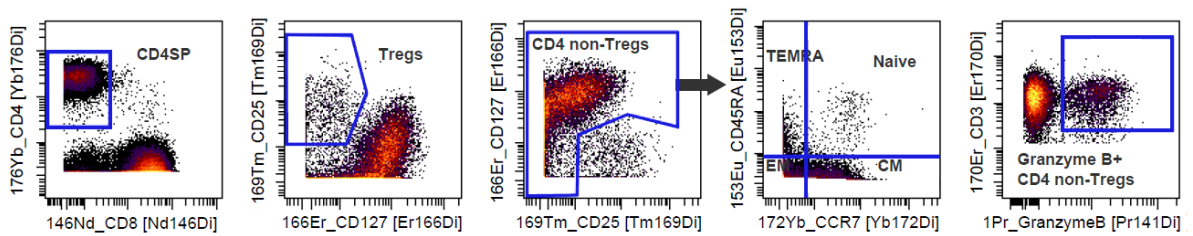
**A CyTOF gating strategy**



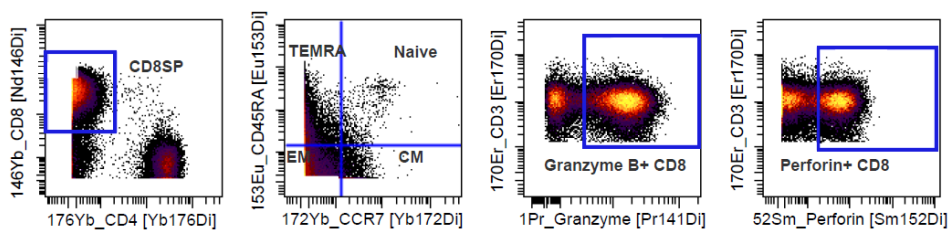
**B Peripheral immune populations**



**C CD4 subsets**

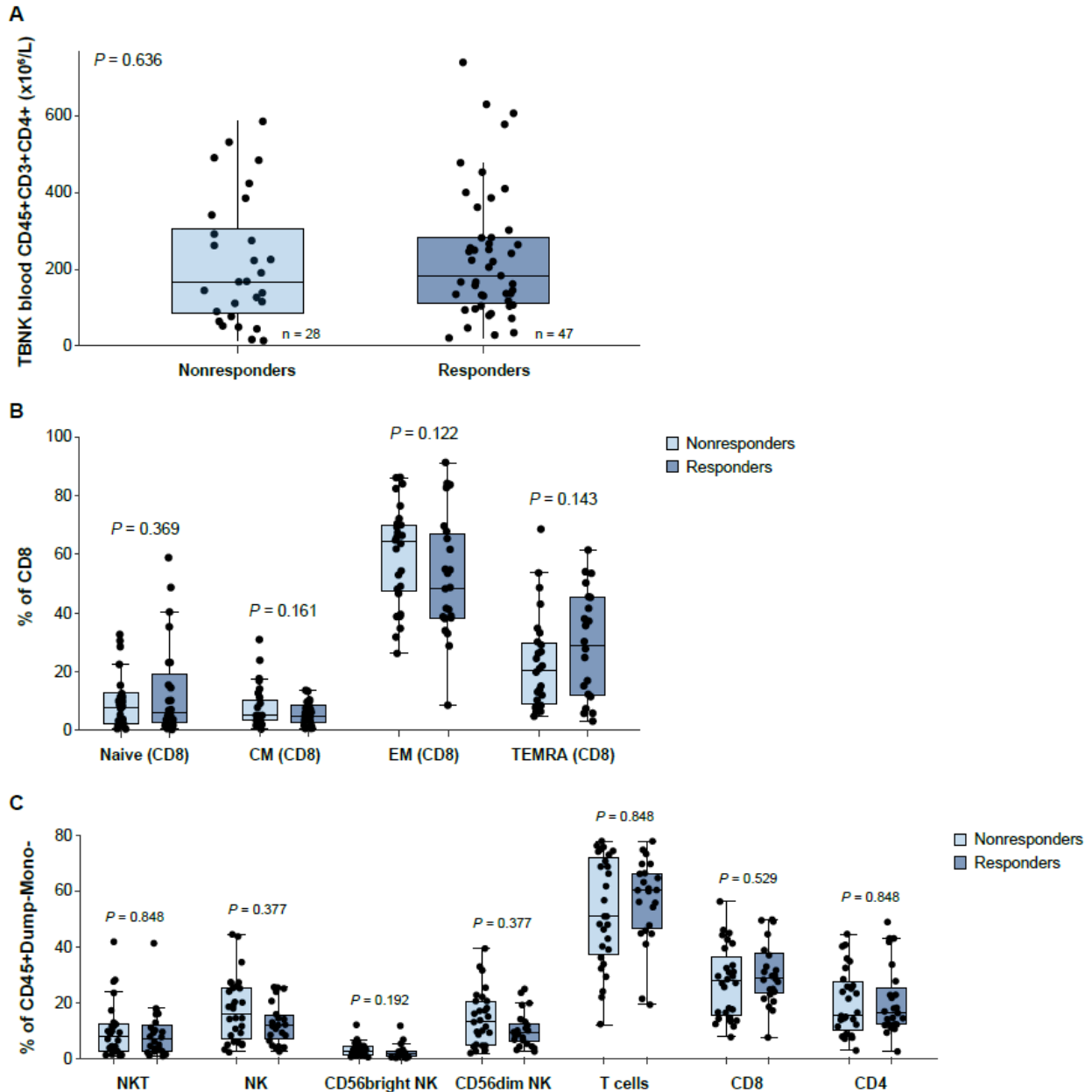


**D CD8 subsets**



(A) Representative dot plots show the gating hierarchy for defining singlet live lymphocytes. (B) Circulating T cells are gated as CD45<sup>+</sup> CD66b<sup>-</sup>CD19<sup>-</sup>CD14<sup>-</sup>CD16<sup>-</sup>CD56<sup>-</sup>CD3<sup>+</sup>, NKT cells as CD45<sup>+</sup> CD66b<sup>-</sup>CD19<sup>-</sup>CD14<sup>-</sup>CD16<sup>-</sup>CD56<sup>-</sup>CD3<sup>+</sup>CD56<sup>+</sup>, while NK cell subsets included CD45<sup>+</sup> CD66b<sup>-</sup>CD19<sup>-</sup>CD14<sup>-</sup>CD16<sup>-</sup>CD56<sup>hi</sup>CD3<sup>-</sup> and CD45<sup>+</sup> CD66b<sup>-</sup>CD19<sup>-</sup>CD14<sup>-</sup>CD16<sup>-</sup>CD56<sup>+</sup>CD3<sup>-</sup>. (C) CD4 T cells were identified as CD45<sup>+</sup> CD66b<sup>-</sup>CD19<sup>-</sup>CD14<sup>-</sup>CD16<sup>-</sup>CD56<sup>-</sup>CD3<sup>+</sup>CD8<sup>-</sup>CD4<sup>+</sup>CD127<sup>all</sup>CD25<sup>-</sup> while Tregs were defined as CD45<sup>+</sup> CD66b<sup>-</sup>CD19<sup>-</sup>CD14<sup>-</sup>CD16<sup>-</sup>CD56<sup>-</sup>CD3<sup>+</sup>CD8<sup>-</sup>CD4<sup>+</sup>CD127<sup>-</sup>CD25<sup>+</sup>. (D) CD8 T cells were identified as CD45<sup>+</sup> CD66b<sup>-</sup>CD19<sup>-</sup>CD14<sup>-</sup>CD16<sup>-</sup>CD56<sup>-</sup>CD3<sup>+</sup>CD8<sup>+</sup>CD4<sup>+</sup>. Data are shown for a representative patient at baseline. CM, central memory; CyTOF, cytometry by time of flight; EM, effector memory; NK, natural killer; NKT, natural killer T cell; TEMRA, terminally differentiated effector memory; Treg, regulatory T cell.

**Supplemental Figure 3. Baseline absolute CD4 T-cell counts by response, and bone marrow memory CD8 T-cell subsets and cellular distribution, in patients from the R2PD cohort of MajesTEC-1.**

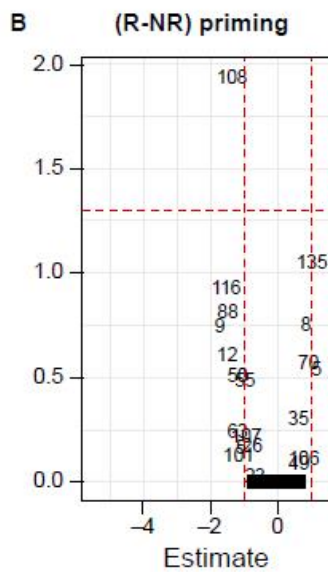
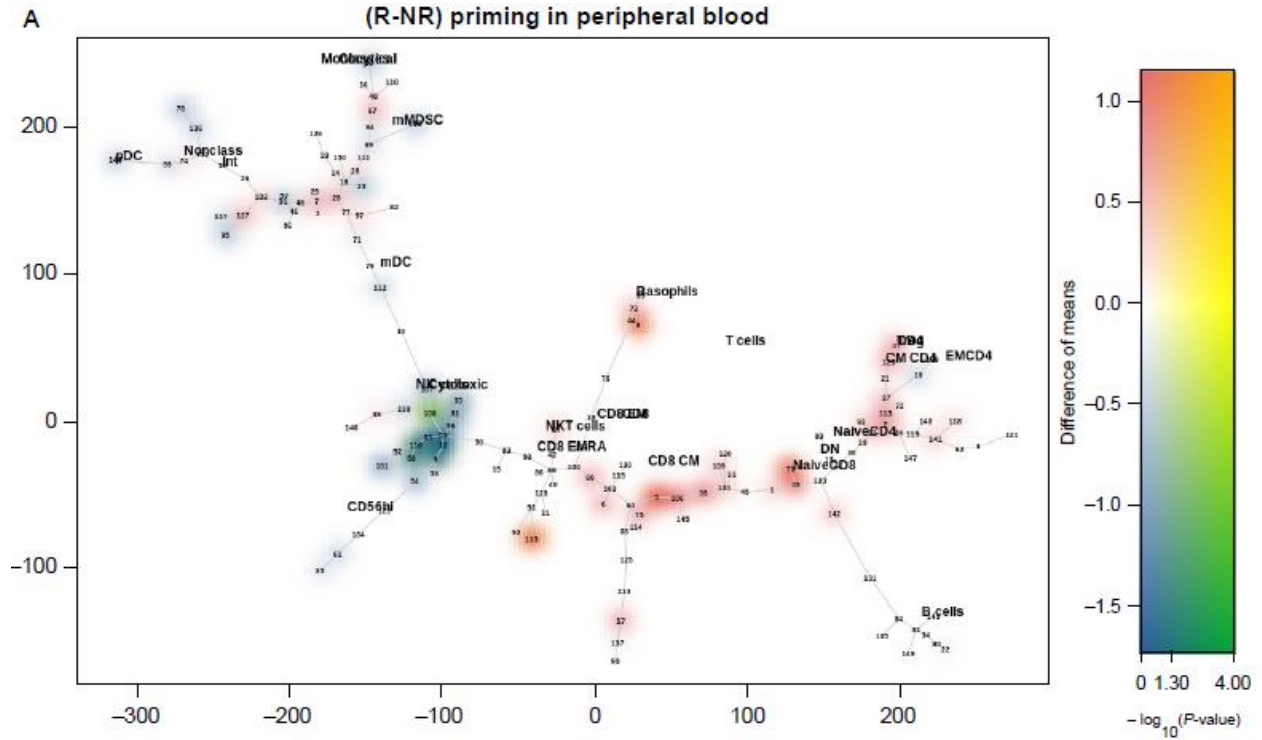


(A) Absolute baseline CD4 T-cell counts assessed by flow cytometry (TBNK kit) relative to response. (B) CD8 T memory subsets from manually gated cell populations at baseline. (C)

Frequencies of manually gated cell populations at baseline from CD138-depleted bone marrow samples relative to response. Data are depicted as box plots and assessed by CyTOF.

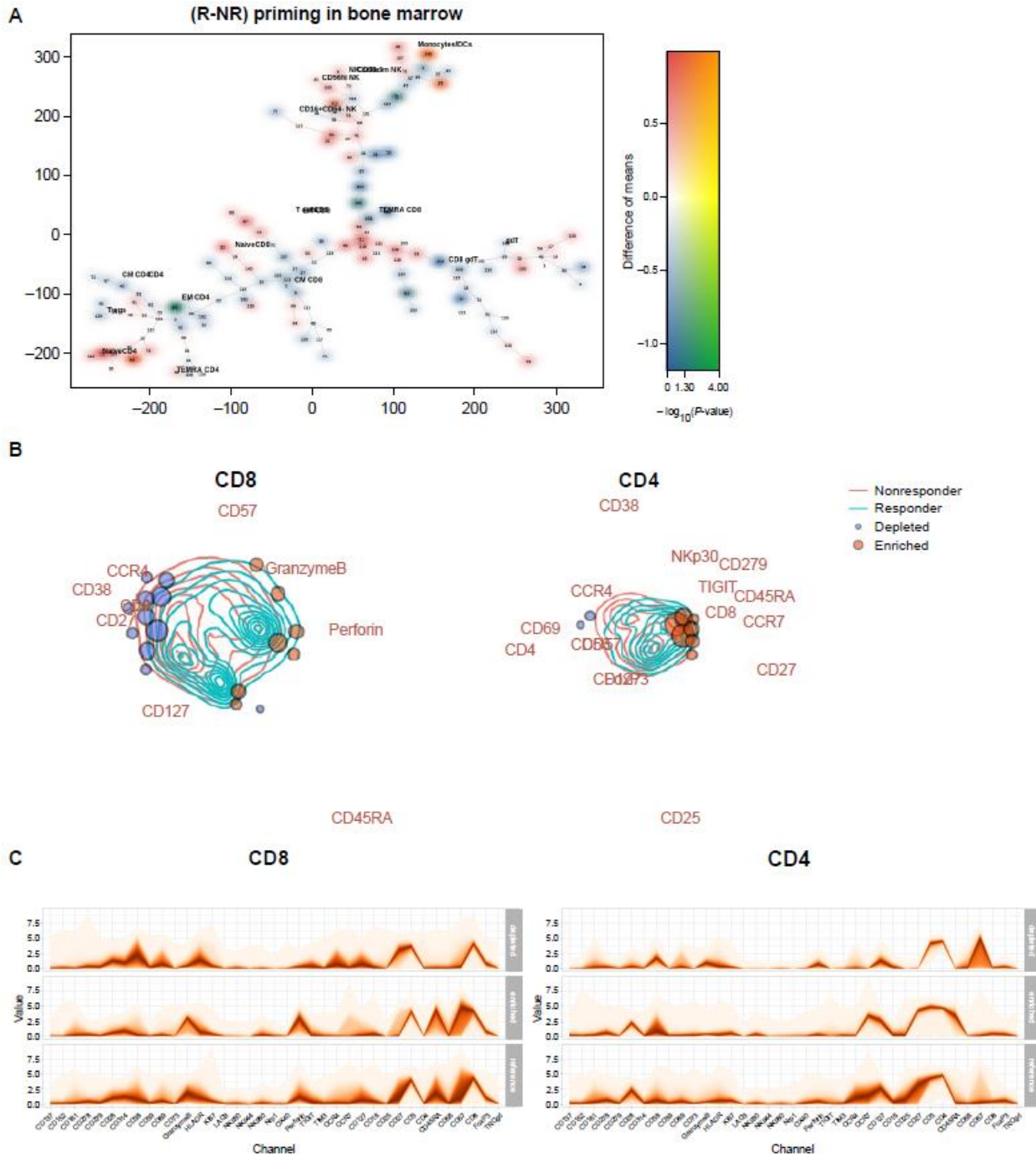
Statistical significance was calculated using the Wilcoxon rank-sum test. Responders were defined as having a best clinical response of partial response or better. CM, central memory; CyTOF, cytometry by time of flight; EM, effector memory; NK, natural killer; NKT, natural killer T cell; RP2D, recommended phase 2 dose; TBNK, T cells, B cells, and natural killer cells; TEMRA, terminally differentiated effector memory.

**Supplemental Figure 4. Characterization of phenotypic and functional differences in immune peripheral blood composition between responders and nonresponders using unsupervised analysis by mass cytometry.**



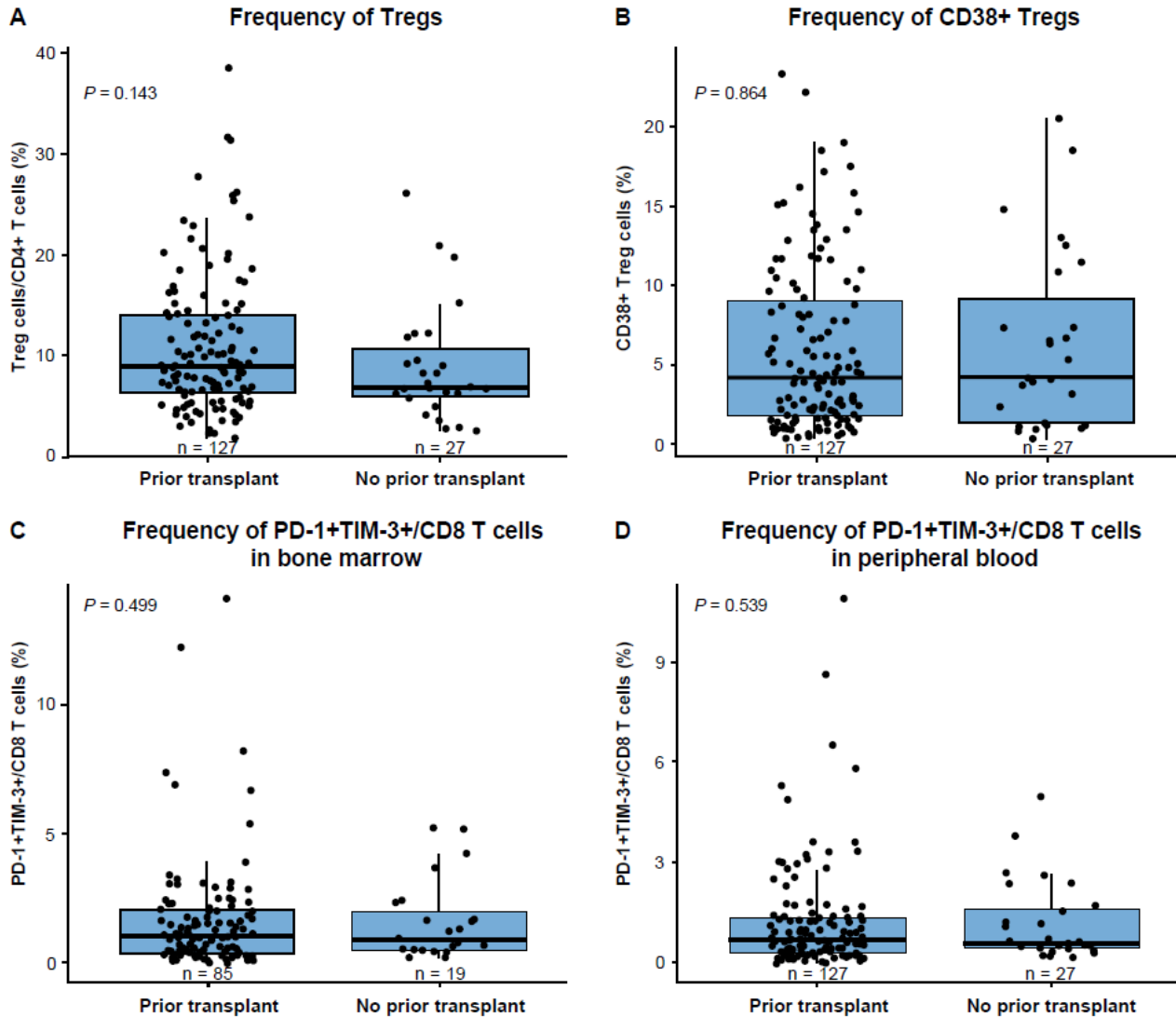
(A) CyTOF analysis of differences in population frequencies between responders and nonresponders visualized by SPADE blend tree. (B) Differential analysis of cluster-based population size shown as a volcano plot. CyTOF, cytometry by time of flight; NR, nonresponder; R, responder; SPADE, Spanning-tree Progression Analysis of Density-normalized Events.

**Supplemental Figure 5. Characterization of phenotypic and functional differences in immune bone marrow composition between responders and nonresponders using unsupervised analysis by mass cytometry.**



(A) CyTOF analysis of differences in population frequencies between responders and nonresponders visualized by SPADE blend tree. (B) FreeViz visualization of functional differences in CD8 (left) and CD4 (right) T-cell composition between responders and nonresponders. (C) Fan plots summarizing phenotypes of CD8 (left) and CD4 (right) T cells enriched and depleted in responders vs nonresponders. CyTOF, cytometry by time of flight; SPADE, Spanning-tree Progression Analysis of Density-normalized Events.

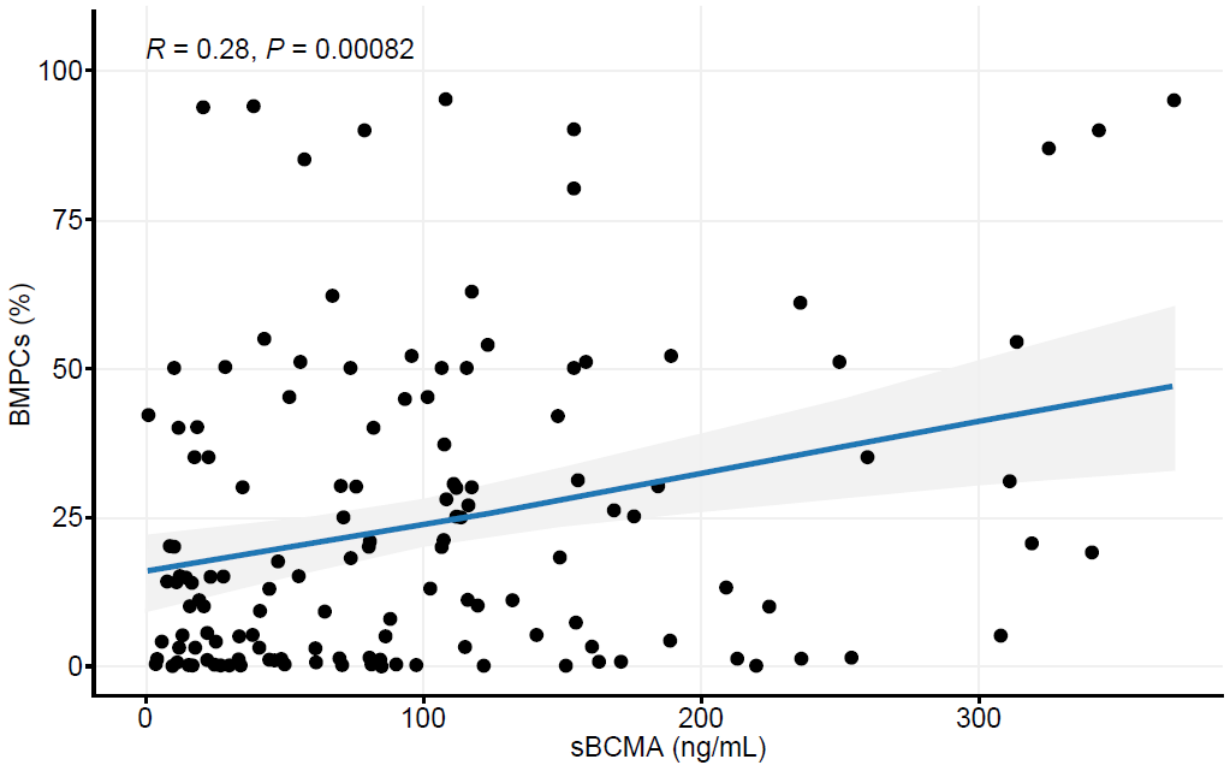
**Supplemental Figure 6. Association of prior transplant with baseline Tregs and bone marrow- and peripheral blood-derived CD8 T cells expressing PD-1 and TIM-3 assessed by flow cytometry.**



(A) Frequency of Tregs in periphery at baseline by prior transplant history. (B) Frequency of peripheral immunosuppressive CD38+ Tregs at baseline by prior transplant history. (C) Frequency of PD-1+TIM-3+/CD8 T cells in bone marrow at baseline by prior transplant history. (D) Frequency of PD-1+TIM-3+/CD8 T cells in peripheral blood at baseline by prior transplant

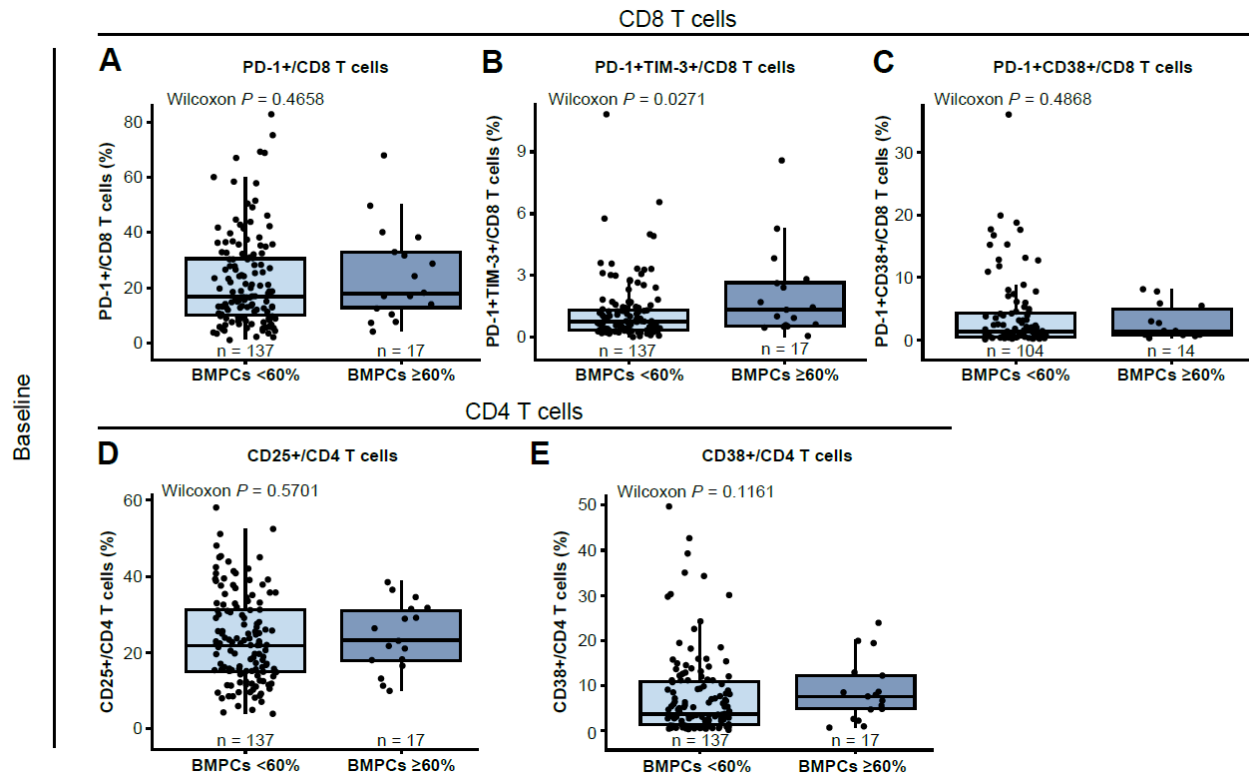
history. Patients with immunoprofiling data and available history on prior transplant were included. Statistical significance was calculated using the Wilcoxon rank-sum test. Treg, regulatory T cell.

**Supplemental Figure 7. Correlation between baseline sBCMA levels and tumor burden (bone marrow BMPC %).**



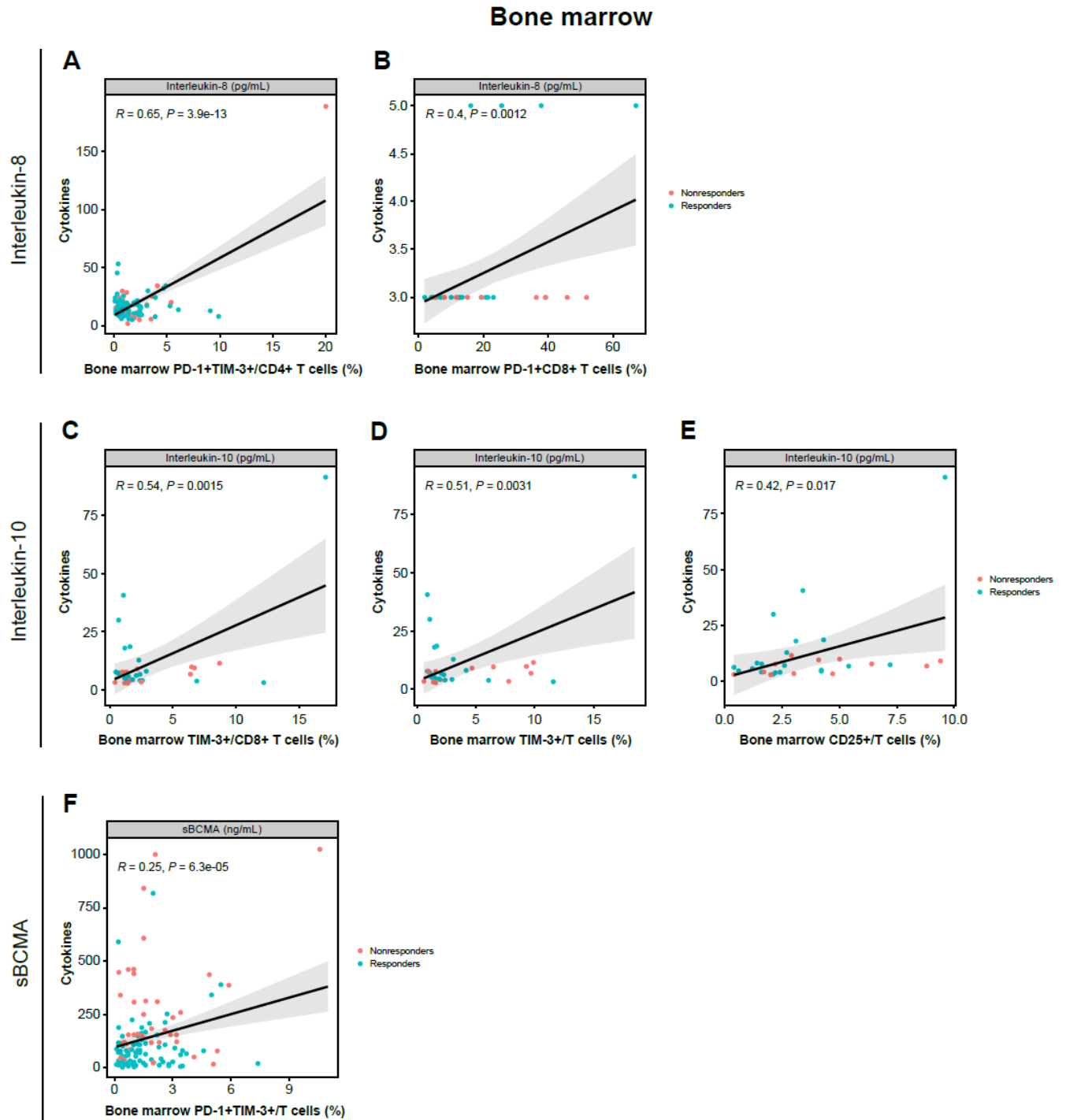
Analysis included 140 patients with available data for baseline serum sBCMA and bone marrow BMPC % (17 outliers detected based on MAD [med-(3MAD), med+(3MAD)] were not included). BMPC, bone marrow plasma cell; MAD, median absolute deviation; sBCMA, soluble B-cell maturation antigen.

**Supplemental Figure 8. Immunophenotypic analyses of T cells at baseline in peripheral blood in relation to disease burden.**

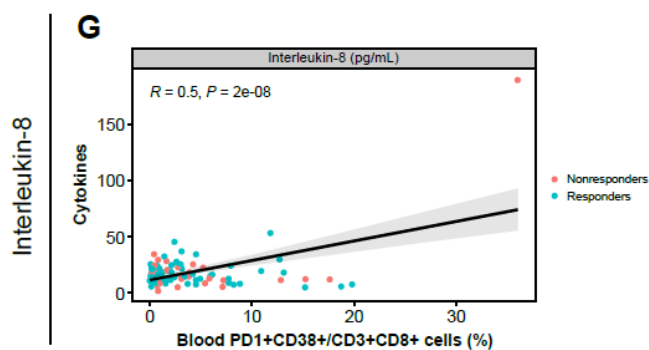


(A-C) Flow cytometry analysis of frequency of PD-1, PD-1/TIM-3, and PD-1/CD38 expression in the CD8 T-cell subset relative to disease burden (percentage of BMPCs) at baseline from the RP2D cohort. (D-E) Flow cytometry analysis of frequency of CD4 T cells expressing CD25 or CD38 at baseline relative to disease burden (percentage of BMPCs) in the RP2D cohort. Statistical analyses were performed using the Wilcoxon rank-sum test. BMPCs, bone marrow plasma cells; RP2D, recommended phase 2 dose.

**Supplemental Figure 9. Linear regression analysis between immune cell populations and serum cytokine levels at baseline in patients from the RP2D cohort of MajesTEC-1.**

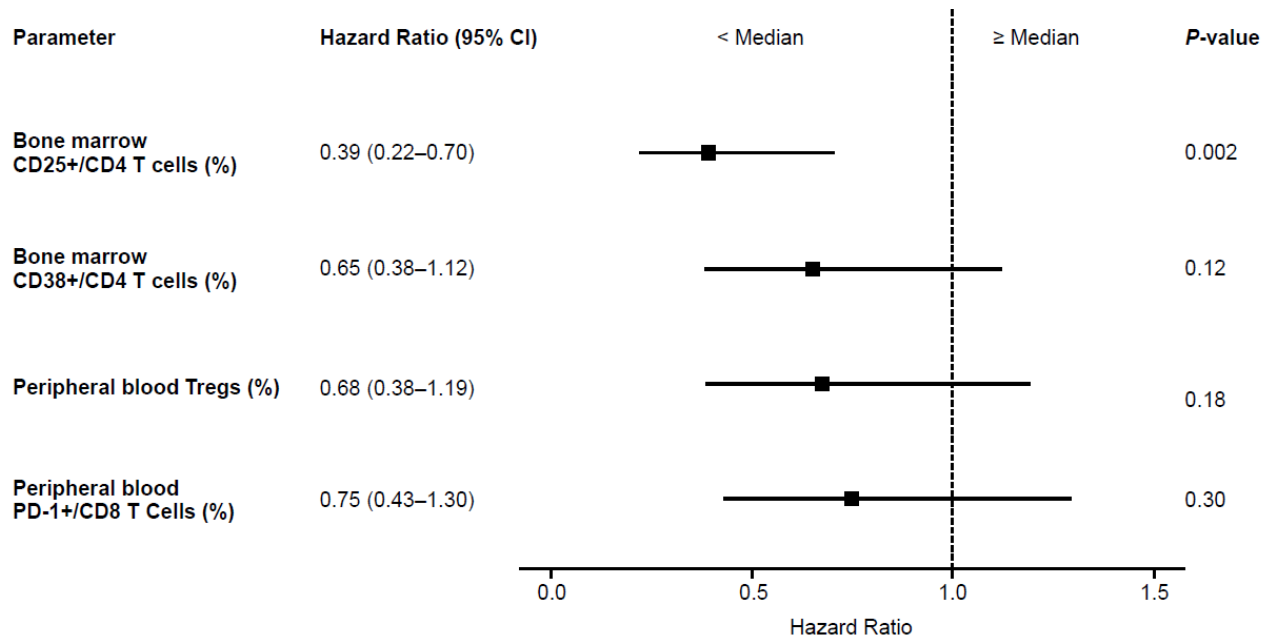


## Peripheral blood



(A) Regression plot of frequency of baseline bone marrow PD-1+TIM-3+/CD4 T cells and serum IL-8. (B) Regression plot of frequency of bone marrow PD-1+/CD8 T cells and serum IL-8. (C-E) Regression plots of frequency of bone marrow TIM-3+/CD8 T cells, TIM-3+/T cells, and CD25+/T cells and serum IL-10. (F) Linear regression curve for sBCMA and bone marrow PD-1+TIM-3+/T cells. (G) Correlation of serum IL-8 and periphery PD-1+CD38+/CD8 T cells. Orange dots represent nonresponders and teal dots represent responders. Responders were defined as having a best clinical response of partial response or better. Black line represents linear regression. IL, interleukin; PD-1, programmed death-1; RP2D, recommended phase 2 dose; sBCMA, soluble B-cell maturation antigen; TIM-3, T-cell immunoglobulin mucin-3.

**Supplemental Figure 10. Forest plot of multivariate Cox regression analysis of key flow cytometry parameters and PFS.**



Patients in the pivotal RP2D cohort with available flow cytometry profiling and PFS data were included. PFS, progression-free survival; RP2D, recommended phase 2 dose.